Indian Journal of Chemical Technology
Vol. 31, July 2024, pp. 647-653
DOI: 10.56042/ijct.v31i4. 9182

Core-shell structure ZrO_2-Al_2O_3 aerogels prepared by one-step drying under constant pressure

Xiaoqing Wang[1]*, Yangyang Wu[1], Gangling Chen[1], Shouquan Zhang[1] & Xinyao Quan[2]*
[1]College of Materials and Chemical Engineering, Chuzhou University, Chuzhou 239000, China
[2]Institute of Agricultural Sciences in Taihu Lake District, Suzhou Academy of Agricultural Sciences, Suzhou 215155, China
*E-mail:xiaoqingwang2013@chzu.edu.cn (XW); quanxinyaoyao@163.com (XQ)

Received 29 February 2024; accepted 29 May 2024

In this work, the monolithic ZrO_2-Al_2O_3 aerogels with hollow sphere structure have been prepared by ambient pressure drying. In the preparation process of Al_2O_3 hollow spheres, different mole of $ZrOCl_2 \cdot 8H_2O$ was added. We explored the maximum addition of zirconium via ambient pressure drying. A series of ZrO_2-Al_2O_3 aerogels with hollow sphere structure are successfully synthesized using $AlCl_3 \cdot 6H_2O$ and $ZrOCl_2 \cdot 8H_2O$ as aluminum and zirconium precursor, and propylene oxide (PO) as the gel initiator by the sol-gel method. It was found that the gelation time was prolonged with increasing zirconium content. When the zirconium content was more than 10%, the gel can't be obtained. It can only get precipitation. With the zirconium content increase from 0 to 10%, the core-shell structure can be formed, proved by SEM and TEM characterizations. The core-shell structure can be kept well under 1000°C. When the heat treatment temperature was at 1200°C, the diffraction peaks were mainly ZrO_2 and Al_2O_3, showed by XRD. With the content of zirconium increase from 0 to 10%, the specific surface area of $XZrO_2$-Al_2O_3-aerogel increased from 170 to 582 m^2/g.

Keywords: Ambient pressure drying, core-shell, hollow sphere, sol-gel, ZrO_2-Al_2O_3

Introduction

Al_2O_3 aerogels have some advantages, such as large specific surface area, low conductivity and high porosity[1, 2]. The heat resistant temperature of Al_2O_3 is up to 1200°C(Ref.3). It's a good candidate for high temperature insulation materials. Al_2O_3 aerogels were used in catalysis, support, thermal management and other fields[4-6].

Traditionally, the morphology of the prepared Al_2O_3 aerogels was almost nanoparticles[7-12]. As we knew, the nanoparticles were apt to sinter, which can lead to the reduced temperature resistance. In order to improve the temperature resistance of Al_2O_3 aerogels, there were two routes which could be implemented. One route was to synthesize different morphologies of Al_2O_3 aerogels. The different morphologies included nanosheets and nanowires, and so on[3,8,13-15]. For example, Shen *et al*. synthesized the rod like and leaf like particles of Al_2O_3-based aerogels[3]. Al_2O_3 aerogels with the mesoporous hollow microspheres were prepared by Fan *et al*. The hollow spheres were made of stacked nanosheets[13]. They all showed good heat resistance at high temperature of 1200°C.

In view of the problem that the Al_2O_3 aerogels would undergo a phase change at a high temperature, it would result in the destruction of its porous structure[16, 17] and it would cause the failure of thermal insulation and mechanical performance. The other route was to synthesize composite aerogels, including Al_2O_3-ZrO_2 aerogels, Al_2O_3-SiO_2 aerogels and so on[11, 14, 18-20]. The addition of a second component can be wrapped around the nanoparticles of Al_2O_3 aerogels, which can restrain the sintering of aerogels. These measurements both can improve the resistance of Al_2O_3 aerogels.

In the second route, the other component of the composite aerogels was traditionally introduced by the aging process or the supercritical fluid drying (SCFD) process[21-24]. For example, the component SiO_2 can be introduced by the aging process or the SCFD process[21-24]. The disadvantage of this introduction method was that the amount was not well controlled. So, some researchers came up with the introduction of ZrO_2 in the synthesis step[14]. But most modification methods used SCFD methods. We knew the supercritical fluid drying technology was time and energy consumption and the high temperature and high pressure in the operation process were dangerous. Compared with SCFD, ambient pressure drying method was convenient, simple and energy saving.

Based on the advantages mentioned above, different content of $ZrOCl_2 \cdot 8H_2O$ were added into $AlCl_3 \cdot 6H_2O$ to synthesize series of core-shell structured ZrO_2-Al_2O_3 aerogels in this work. The gelation time, formation a gel or precipitate, its morphology and crystallization were researched. The largest proportion of zirconium to aluminum that can form gel under atmospheric drying conditions was obtained under the conditions we set for the experiments. The obtained ZrO_2-Al_2O_3 aerogels had core-shell structure characterized by SEM and TEM. The size of ZrO_2 core got bigger with the content of zirconium increase characterized by SEM. The existence of ZrO_2 would affect the phase transformation of Al_2O_3 and inhabit the appearance of new Al_2O_3 phase at 1200°C characterized by XRD.

Experimental Section

Materials

All chemical reagents were analytically pure and were used as received without further purification.

Characterization

HITACHIS-4800 scanning electron microscope (SEM), the EDX data were characterized by SEM instrument JSM-6510LV made by Japan Electronics Co., LTD, and transmission electron microscope (TEM: JEM-1200EX, JEOL, Japan) were used to characterize the microstructure of the prepared aerogels. Crystallization condition of the aerogels was characterized in a X-ray diffractometer (X'Pert PRO, PANalytical B.V.) with the use of Cu K_α radiation (λ = 1.5418Å) at 4° min^{-1} scanning speed in the 2θ range from 10-80° by X-ray diffraction (XRD) measurements. Surface area and the pore size distributions were evaluated by the Brunauer-Emmett-Teller (BET) method and the Barrett-Joyner-Halenda (BJH) model, respectively. The average pore diameters and cumulative pore volumes were calculated using the adsorption branch of the isotherm. The data of nitrogen adsorption-desorption isotherms were measured by instruments manufactured by Quantachrome Instrument Corp were obtained at 77 K. Thermogravimetric analysis (TGA) and differential thermal analysis (DTA) were performed on a SDT-Q 600TGA instrument. The samples were heated from room temperature to 1000°C at 10°C/min.

Synthesis of ZrO_2-Al_2O_3 aerogels

We referred the preparation parameters as per the available literature[13]. Take the sample for example. In the preparation of $0.02ZrO_2$-Al_2O_3 sample, the precursor $ZrOCl_2 \cdot 8H_2O$ (0.08 g) and $AlCl_3 \cdot 6H_2O$ (2.83 g) were mixed with ethanol (3.60 mL) and deionized water solution (2.60 mL) and the mixed solution was kept stirring until it became clear. Then 5 mL of PO was added into the precursor solution, and kept stirring for 1 min. The magnet was taken out and sealed at 60°C to form the wet gel. The gelation time of the samples was recorded. After the wet gels formed, Oswald was matured for 2 h. Then aged the wet gels with isopropyl alcohol for 3 days, and changed every six hours. At last the wet gels were dried under atmospheric pressure in a blast drying oven at 50°C. The remaining $XZrO_2$-Al_2O_3-aerogel (X = 0, 0.04, 0.06, 0.08, 0.1) samples were synthesized in the same way. Table 1 showed the preparation parameters of all samples.

Results and Discussion

To obtain monolithic ZrO_2-Al_2O_3 composite aerogels under atmospheric drying, different ratios of $AlCl_3 \cdot 6H_2O$ and $ZrOCl_2 \cdot 8H_2O$ were regulated. From Table 1, it can be seen that the gelation time of pure Al_2O_3 was 7 min, while $0.1ZrO_2$-Al_2O_3 was 99 min. Compared with the data in Table 1, it can be easily obtained that the gelation time was prolonged with increased zirconium content. When the molar ratio of Zr^{4+} was up to 12%, the gel cannot be formed. It may be attributed to the special structure of Zr, that it cannot be formed three dimensional structure alone.

The photographs of the aerogels prepared were given in Fig. S1 (Supplementary Information). From

Table 1 — Synthesis parameters of the ZrO_2-Al_2O_3 aerogels

Samples	$n(Al^{3+})$: $n(Zr^{4+})$	$m(AlCl_3 \cdot 6H_2O)$/g	$m(ZrOCl_2 \cdot 8H_2O)$/g	V_{H2O}/mL	V_{EtOH}/mL	V_{PO}/mL	gelation time/min
Al_2O_3	100:0	3.00	0	2.80	3.80	5	7
$0.02ZrO_2$-Al_2O_3	98:2	2.83	0.08	2.60	3.60	5	21
$0.04ZrO_2$-Al_2O_3	96:4	2.78	0.15	2.50	3.50	5	22
$0.06ZrO_2$-Al_2O_3	94:6	2.72	0.23	2.46	3.40	5	69
$0.08ZrO_2$-Al_2O_3	92:8	2.66	0.31	2.40	3.36	5	72
$0.1ZrO_2$-Al_2O_3	90:10	2.60	0.39	2.30	3.20	5	99
$0.12ZrO_2$-Al_2O_3	88:12	2.54	0.46	2.26	3.16	5	/

the photographs, we saw the integrity of the synthesized samples, and the diameter of the monolithic aerogels was about 4 cm.

The SEM images of the prepared aerogels are shown in Fig. 1 (a and b) and Fig. 2. In order to demonstrate the light weight of the prepared aerogels, the Al_2O_3 sample was put in a leaf of Chinese ilex, seen in Fig. 1c. The morphology of $XZrO_2$-Al_2O_3-aerogel (X = 0, 0.02, 0.04, 0.06, 0.08, 0.1) as-prepared was hollow sphere and the size of the hollow sphere was about 2-4 μm. The hollow spheres were made of nanosheets. Compared with the images (a) to (e) in Fig. 2, it can be concluded that with the increase of zirconium content, zirconium spheres would appear inside alumina hollow spheres and the zirconium spheres were getting bigger and bigger. When the zirconium content was more than 10%, the gel cannot be formed. The micromorphology of aerogels was a mixture of broken nanosheets and nanospheres, seen in Fig. 2f. The EDX data were shown in Fig. S3, and the atom ratio of Al/Zr was seen in Table S1. On account of the added zirconium content being too low, and the selected area being relatively small (seen in Fig. S3), the atom ratio of Al/Zr was not accurate. Therefore, it was not in agreement with the feed ratio.

When the sample $0.1ZrO_2$-Al_2O_3-aerogel was treated at 1000℃, the morphology of the hollow spheres can be basically maintained, seen in Fig. 3a. While it was heat treated at 1200℃, most of the hollow spheres would sinter and stick together, seen in Fig. 3b. It indicated that the composite hollow spheres prepared at 1000℃ had relatively good thermal stability, while it had poor thermal stability at 1200℃. The shrinkage of the sample after heat treatment can also explain this phenomenon. The detailed data were listed in Fig. S2 and Table 2. After

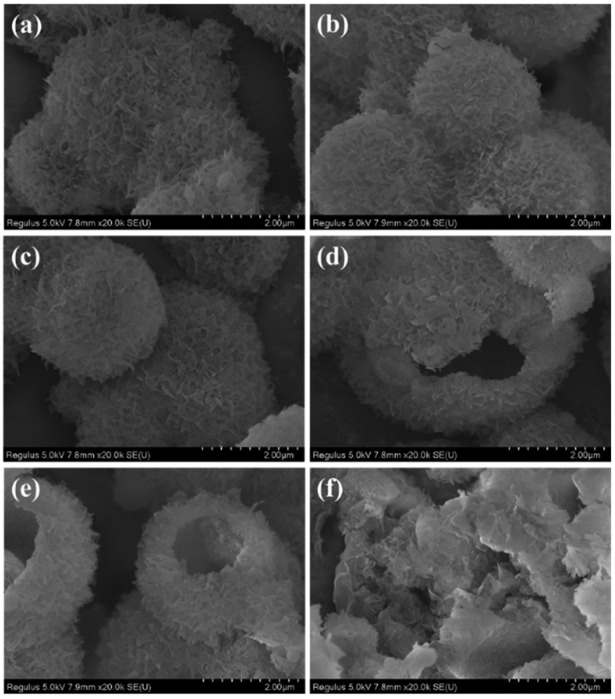

Fig. 2 — (a)-(f) SEM images of different composite aerogels samples $XZrO_2$-Al_2O_3-aerogel (X = 0.02, 0.04, 0.06, 0.08, 0.1, 0.12)

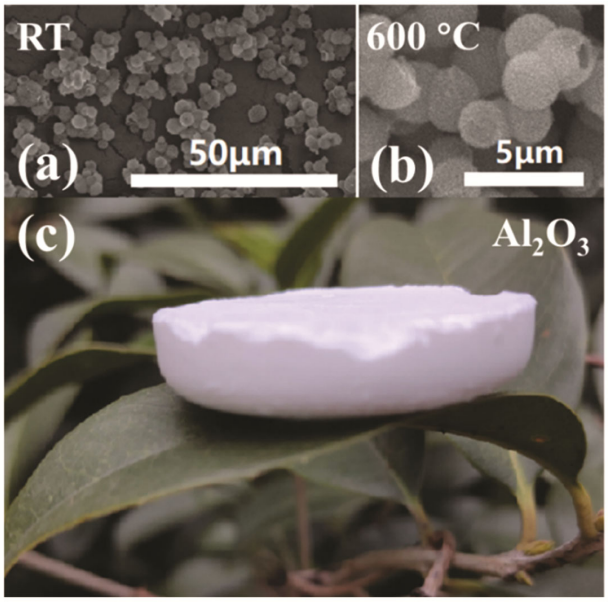

Fig. 1 — SEM images of Al_2O_3 aerogel sample: (a) Al_2O_3-RT, (b) Al_2O_3-600 ℃, (c) photograph of Al_2O_3

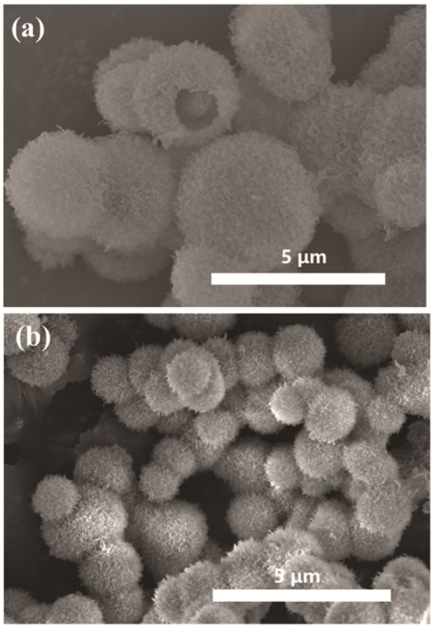

Fig. 3 — SEM images of (a) aerogel sample $0.1ZrO_2$-Al_2O_3-aerogel-1000 and (b) $0.1ZrO_2$-Al_2O_3-aerogel-1200

Table 2 — Surface area, pore volume and linear shrinkage of $XZrO_2$-Al_2O_3-aerogel as-prepared and that treated at 1200°C

Samples	Surface area (m^2/g)	Pore volume (cm^3/g)	Linear shrinkage (ΔL/L)	Density(g/m^3)
Al_2O_3	170	1.05	/	0.1051
Al_2O_3-1200	/	/	36.17%	0.1679
0.02ZrO_2-Al_2O_3	226	0.92	/	0.0922
0.02ZrO_2-Al_2O_3-1200	/	/	/	0.1821
0.04ZrO_2-Al_2O_3	252	1.06	/	0.09595
0.04ZrO_2-$Al_2O_3$1200	/	/	34.68%	0.2190
0.06ZrO_2-Al_2O_3	482	1.37	/	0.09716
0.06ZrO_2-Al_2O_3-1200	/	/	34.53%	0.1954
0.08ZrO_2-Al_2O_3	482	1.15	/	0.09945
0.08ZrO_2-Al_2O_3-1200	/	/	/	0.1952
0.1ZrO_2-Al_2O_3	582	1.43	/	0.1329

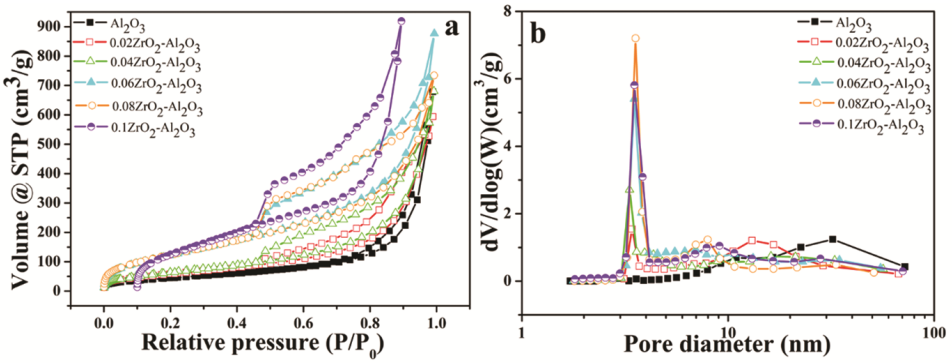

Fig. 4 — (a) N_2 adsorption-desorption isotherms of $XZrO_2$-Al_2O_3-aerogel and (b) their pore size distribution curves at room temperature

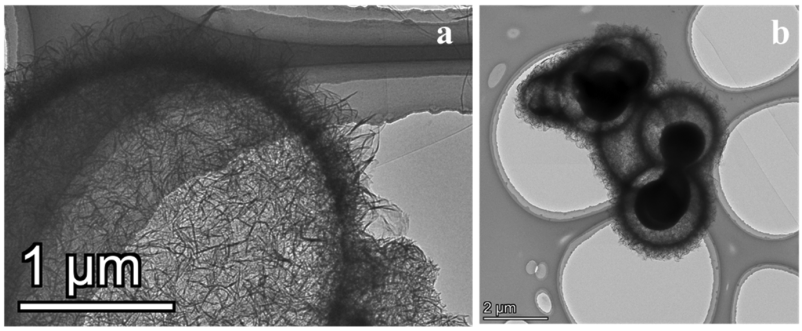

Fig. 5 — The TEM image of the aerogel samples (a) Al_2O_3-aerogeland (b) 0.1ZrO_2-Al_2O_3-aeroge

treatment at 1200℃, the size of the aerogels was about 3 cm. It was smaller than that before the treatment. The shrinkage rate was about 35%. The shrinkage of 0.1ZrO_2-Al_2O_3-aerogel at 1200℃ was 33.45%, and it was the smallest among all the samples. It indicated the addition of zirconium played an important role in inhibiting the shrinkage of composite aerogels. It can also be explained in the following XRD characterization.

N_2 adsorption-desorption characterizations were applied to study the specific surface area and pore volume of $XZrO_2$-Al_2O_3-aerogel (X = 0, 0.02, 0.04, 0.06, 0.08, 0.1).The detailed data were listed in Table 2. From Table 2, it can be seen that with the amount of ZrO_2 increase, the specific surface area of aerogels augmented. Fig. 4a showed the isotherm curves of aerogel with different amount of ZrO_2, which can be seen as type II curves, indicating the existence of large pores in the samples. The pore diameter of the most samples was less than 10 nm, shown in Fig. 4b. The specific surface area of 0.1ZrO_2-Al_2O_3-aerogel was 582 m^2/g and its pore volume was 1.43 cm^3/g. 0.1ZrO_2-Al_2O_3-aerogel was the best sample among our prepared samples.

The TEM images of the aerogel samples Al_2O_3-aerogel and 0.1ZrO_2-Al_2O_3-aerogel were shown in Fig. 5. From the images it can be seen that ZrO_2 and Al_2O_3 can form the core-shell structure. The shell was

Al_2O_3 hollow sphere, which was made of nanosheets, shown in Fig. 5a. This structure was the same with the reported literature[13, 14]. The size of the hollow sphere was about 2-4 μm, corresponding with the results characterized by SEM. The core was ZrO_2 solid spheres, and its size was about 1-2 μm, the dark solid ball shown in Fig. 5b. With the zirconium salt adding, a core appeared inside the hollow Al_2O_3 spheres. It was consistent with the SEM results.

The XRD images of the aerogel samples $XZrO_2$-Al_2O_3-aerogel (X = 0, 0.02, 0.04, 0.06, 0.08, 0.1) treated at 600°C, 800°C, 1000°C and 1200°C were displayed in Fig. 6. From the images it can be easily seen that the diffraction peak intensity increased with

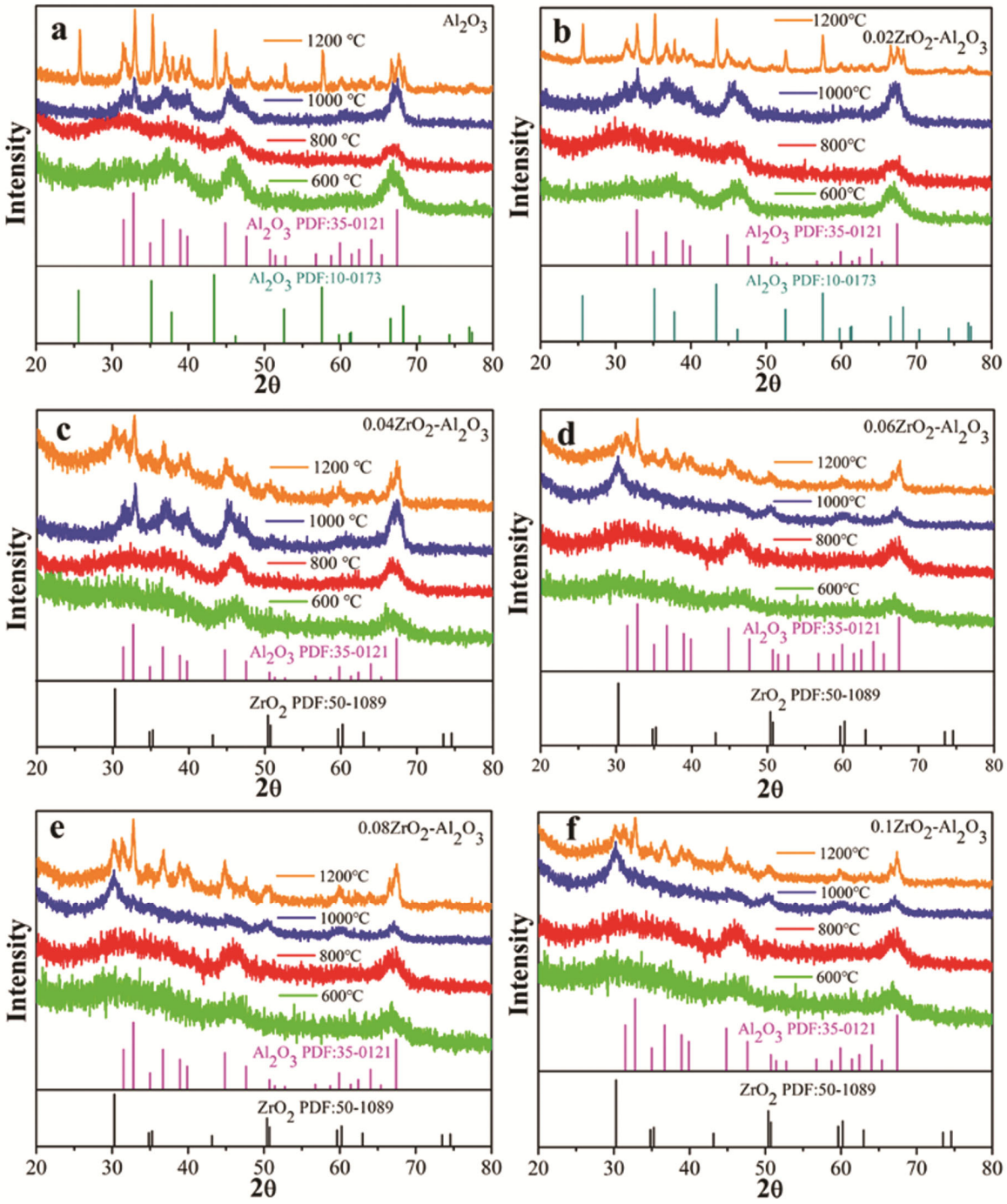

Fig. 6 — (a-f) The XRD images of the aerogel samples $XZrO_2$-Al_2O_3-aerogel (X = 0, 0.02, 0.04, 0.06, 0.08, 0.1) treated at 600 °C, 800 °C, 1000 °C and 1200 °C

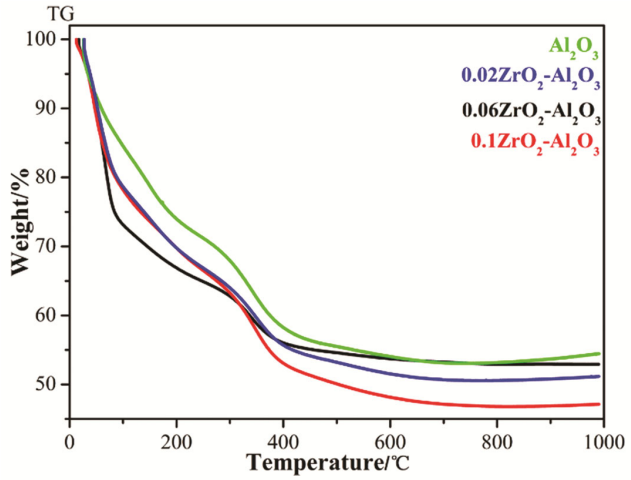

Fig. 7 — TGA curves of aerogels of the samples $XZrO_2$-Al_2O_3 (X = 0, 0.02, 0.06, 0.1)

the increase of temperature. When the heat treatment temperature was under 1000°C, there was only Al_2O_3 (PDF card: 35-0121), and the diffraction peaks were weak. When the heat treatment temperature was at 1000°C, there was only Al_2O_3 (PDF card: 35-0121) in samples Al_2O_3-aerogel, $0.02ZrO_2$-Al_2O_3-aerogel and $0.04ZrO_2$-Al_2O_3-aerogel, seen in Fig. 6 (a, b and c). While ZrO_2 phase (PDF card: 50-1089) appeared at 1000°C in samples $0.06ZrO_2$-Al_2O_3-aerogel, $0.08ZrO_2$-Al_2O_3-aerogel and $0.1ZrO_2$-Al_2O_3-aerogel, seen in Fig. 6 (d, e and f). When the heat treatment temperature was at 1200°C, the phase transition occurred, and a new diffraction peak of Al_2O_3 appeared (PDF card: 10-0173) in samples Al_2O_3-aerogel and $0.02ZrO_2$-Al_2O_3-aerogel, seen in Fig. 6 (a and b). While there was no new Al_2O_3 phase in other samples, seen in Fig. 6 (c, d, e and f). It can be explained that the phase transition of Al_2O_3 can be inhibited by adding appropriate zirconia[25]. When the temperature was at 1200°C, the hollow Al_2O_3 spheres were reduced in size and sintered together. It can be proved by SEM (Fig. 3b). Therefore, it can be concluded that the phase transition of Al_2O_3 can be inhibited at 1200°C when $n(Al^{3+})$: $n(Zr^{4+})$ was 96:4, 94:6, 92:8 and 90:10.

Fig. 7 showed the TGA result of the synthesized samples $XZrO_2$-Al_2O_3 (X = 0, 0.02, 0.06, 0.1). The samples were lost about 15-25 wt% weight loss at the temperature lower than 200°C, corresponding to the surface adsorbed water and part of organics on the particles surface. There was about 20-30 wt% weight loss from 200 to 600 °C, which was mainly attributed to the decomposition of residual organics. And there was almost no weight loss from 600 to 1000°C, indicating that the remaining materials were ZrO_2 and Al_2O_3. According to the added materials of $m(AlCl_3 \cdot 6H_2O)$ and $m(ZrOCl_2 \cdot 8H_2O)$, the total mass of the converted Al_2O_3 and ZrO_2 were 1.267 g, 1.226 g, 1.237 g, 1.247 g, respectively. It was basically in agreement with the results of TGA curves in Fig. 7 except for the sample $0.1ZrO_2$-Al_2O_3. This may be related to the fact that close to the critical value, the added zirconium salts did not all form hollow spherical structures with aluminum salts.

Conclusion

In summary, a series of core-shell structured ZrO_2-Al_2O_3 aerogels were synthesized by one-step sol-gel method under constant pressure drying. It was found that with the zirconium salt added, zirconium core appeared inside the hollow Al_2O_3 sphere. When $n(Al^{3+})$: $n(Zr^{4+})$ was higher than 90:10, there was no gel formation under the conditions we set for the experiments. With the increase of zirconium content, the core-shell structure was gradually obvious, characterized by SEM and TEM; and the specific surface area of $XZrO_2$-Al_2O_3-aerogel increased from 170 to 582 m^2/g, represented by N_2 adsorption-desorption characterization. The core-shell structure can keep well under 1000°C. When the temperature was 1200°C, the outside shell Al_2O_3 would reduce in size and sinter together, characterized by SEM. There was no new diffraction peak of Al_2O_3 at 1200°C when $n(Al^{3+})$: $n(Zr^{4+})$ was 96:4, 94:6, 92:8 and 90:10. It demonstrated that the phase transformation was inhabited with appropriate zirconium salt addition, characterized by XRD.

Acknowledgements

This work is supported by National Natural Science Foundation of China (Grant No.22109017), General Natural Science Research Projects of Colleges and Universities in Anhui Province (Grant No. KJ2021B14), Anhui Provincial Science and Technology Key R&D Program (Grant No. 2022a05020055), Natural Science Foundation of the Anhui Higher Education Institutions (2023AH030096 and 2022AH051086), "Double Creation Star" Industry Innovation Team – Key Technology Research on New Membrane Materials (Project Number: 00002606).

Supplementary Information

Supplementary information is available on the website http://nopr.niscpr.res.in/handle/123456789.

References

1 Zu G, Shen, J, Wei X, Ni X, Zhang Z, Wang J & Liu G, Preparation and characterization of monolithic alumina aerogels, *J Non-cryst Solids*, 357 (2011) 2903.

2 Zeng D J, Zhang H H, Yang J F, Wang B & Zhang X L, Microstructure and property of porous mullites with a whiskers framework obtained by a sol-gel process, *Ceram Int*, 42 (2016) 11270.

3 Zu G, Shen J, Zou L, Wang W, Lian Y, Zhang Z & Du A, Nanoengineering super heat-resistant, strong alumina aerogels, *Chem Mater*, 25 (2013) 4757.

4 Pakharukova V P, Shalygin A S, Gerasimov E Y, Tsybulya S V & Martyanov O N, Structure and morphology evolution of silica-modified pseudoboehmite aerogels during heat treatment, *J Solid State Chem*, 233 (2016) 294.

5 Liu F, Jiang Y, Feng J, Li L & Feng J, Bionic aerogel with a lotus leaf-like structure for efficient oil-water separation and electromagnetic interference shielding, *Gels*, 9 (2023) 214.

6 Yu X, Ren X, Wang X, Tang G H & Du M, A high thermal stability core-shell aerogel structure for high-temperature solar thermal conversion, *Compos Commun*, 37 (2023) 101440.

7 Ji L, Lin J, Tan K L & Zeng H C, Synthesis of high-surface-area alumina using aluminum tri-sec-butoxide-2,4-pentanedione-2-propanol-nitric acid precursors, *Chem Mater*, 12 (2000) 931.

8 Poco J F, Satcher J H, Hrubesh L W, Poco J F, Satcher J H & Hrubesh LW, Synthesis of high porosity, monolithic alumina aerogels, *J Noncryst Solids*, 285 (2001) 57.

9 Tokudome Y, Fujita K, Nakanishi K, Kanamori K, Miura K, Hirao K & Hanada T, Sol-gel synthesis of macroporous YAG from ionic precursors via phase separation route, *J Ceram Soc Japan*, 115 (2007) 925.

10 Tokudome Y, Nakanishi K, Kanamori K, Fujita K, Akamatsu H & Hanada T, Structural characterization of hierarchically porous alumina aerogel and xerogel monoliths, *J Colloid Interf Sci*, 338 (2009) 506.

11 Zhao W, Ji Y, Pang Y, Li X & Ji H, Preparation of Al_2O_3-SiO_2aerogel by ambient pressure drying for thermal insulation application, *J Porous Mater*, 30 (2023) 1753.

12 Ang J, Wang Q, Wang T & Liang Y, Rapid preparation process, structure and thermal stability of lanthanum doped alumina aerogels with a high specific surface area, *RSC Adv*, 6 (2016) 26271.

13 Wu L, Qiao X, Cui S, Hong Z & Fan X, Synthesis of monolithic aerogel-like alumina via the accumulation of mesoporous hollow microspheres, *Micropor Mesopor Mater*, 202 (2015) 234.

14 Shi Z, Gao H, Wang X, Li C, Wang W, Hong Z & Zhi M, One-step synthesis of monolithic micro-nano yttria stabilized ZrO_2-Al_2O_3 composite aerogel, *Micropor Mesopor Mater*, 259 (2018) 26.

15 Pakharukova V P, Shalygin A S, Gerasimov E Y, Tsybulya S V & Martyanov O N, Structure and morphology evolution of silica-modified pseudoboehmite aerogels during heat treatment, *J Solid State Chem*, 233 (2016) 294.

16 Wen S, Ren H, Zhu J, Bi Y & Zhang L, Fabrication of Al_2O_3 aerogel-SiO_2 fiber composite with enhanced thermal insulation and high heat resistance, *J Porous Mater*, 26 (2018) 1027.

17 Yang J, Wang Q, Wang T & Liang Y, Facile one-step precursor-to-aerogel synthesis of silica-doped alumina aerogels with high specific surface area at elevated temperatures, *J Porous Mater*, 24 (2016) 889.

18 Xia C, Hao M, Liu W, Zhang X, Miao Y, Ma C & Gao F, Synthesis of Al_2O_3-SiO_2 aerogel from water glass with high thermal stability and low thermal conductivity, *J Sol-gel Sci Technol*, 106 (2023) 561.

19 Chen H, Sui X Y, Zhou C L, Wang C H & Liu F T, Preparation and characterization of monolithic Al_2O_3-SiO_2 aerogel, *J Ceram Soc Japan*, 124 (2016) 442.

20 Aravind P R, Mukundan P, Krishna P P & Warrier K G K, Mesoporous silica-alumina aerogels with high thermal pore stability through hybrid sol-gel route followed by subcritical drying, *Micropor Mesopor Mater*, 96 (2006) 14.

21 Zu G, Shen J, Wang W, Zou L, Lian Y, Zhang Z, Liu B & Zhang F, Robust, highly thermally stable, core-shell nanostructured metal oxide aerogels as high-temperature thermal superinsulators, adsorbents, and catalysts, *Chem Mater*, 26 (2014) 5761.

22 Wang Q, Li X, Fen W, Ji H, Sun X & Xiong R, Synthesis of crack-free monolithic ZrO_2 aerogel modified by SiO_2, *J Porous Mater*, 21 (2014) 127.

23 Hu Z, He J, Li X, Ji H, Su D & Qiao Y, Improvement of thermal stability of ZrO_2-SiO_2 aerogels by an inorganic-organic synergetic surface modification, *J Porous Mater*, 24 (2016) 657.

24 Xiong R, Li X, Ji H, Sun X & He J, Thermal stability of ZrO_2-SiO_2 aerogel modified by Fe(III) ion, *J Sol-gel Sci Technol*, 72 (2014) 496.

25 Al-Yassir N & Le V M R, Thermal stability of alumina aerogel doped with yttrium oxide, used as a catalyst support for the thermocatalytic cracking (TCC) process: An investigation of its textural and structural properties, *Appl Catal A*, 317 (2007) 275.